IEEE Access
Multidisciplinary | Rapid Review | Open Access Journal

Received June 25, 2021, accepted July 11, 2021, date of publication July 20, 2021, date of current version August 9, 2021.

Digital Object Identifier 10.1109/ACCESS.2021.3098453

Identifying Patients With PTSD Utilizing Resting-State fMRI Data and Neural Network Approach

MIRZA NAVEED SHAHZAD[1], HAIDER ALI[1], TANZILA SABA[2], (Senior Member, IEEE), AMJAD REHMAN[2], (Senior Member, IEEE), HOSHANG KOLIVAND[3,4], AND SAEED ALI BAHAJ[5]

[1]Department of Statistics, University of Gujrat, Gujrat 50700, Pakistan
[2]Artificial Intelligence & Data Analytics Lab (AIDA), CCIS, Prince Sultan University, Riyadh 12435, Saudi Arabia
[3]School of Computer Science and Mathematics, Liverpool John Moores University, Liverpool L2 2QP, U.K.
[4]School of Computing and Digital Technologies, Staffordshire University, Staffordshire ST4 2DE, U.K.
[5]MIS Department, College of Business Administration, Prince Sattam Bin Abdulaziz University, Alkharj 16278, Saudi Arabia

Corresponding author: Mirza Naveed Shahzad (nvd.shzd@uog.edu.pk), Tanzila Saba (drstanzila@gmail.com), and Saeed Ali Bahaj (s.bahaj@psau.edu.sa)

This work was supported in part by the University of Gujrat, Gujrat, Pakistan, and in part by the Artificial Intelligence & Data Analytics Lab (AIDA), College of Computer and Information Sciences (CCIS), Prince Sultan University, Riyadh, Saudi Arabia.

Data used in preparation of this article were obtained from the Alzheimer's Disease Neuroimaging Initiative (ADNI) database (adni.loni.usc.edu). As such, the investigators within the ADNI contributed to the design and implementation of ADNI and/or provided data but did not participate in analysis or writing of this report. A complete listing of ADNI investigators can be found at: http://adni.loni.usc.edu/wp-content/uploads/how_to_apply/ADNI_Acknowledgement_List.pdf

ABSTRACT **Purpose**: The primary aim of the study is to identify the existence of post-traumatic stress disorder (PTSD) in an individual and to detect the dominance level of each affected brain region in PTSD using rs-fMRI data. This will assist the psychiatrists and neurologists to distinguish impartially between PTSD individuals and healthy controls for the brain-based treatment of PTSD. **Methods**: Twenty-eight individuals (14 with PTSD, 14 healthy controls) were assessed to obtain rs-fMRI data of their six brain regions-of-interest. The rs-fMRI data analyzed by the Artificial Neural Network (ANN), adopting the training-validation-testing approach to classify PTSD and to identify the most affected brain region due to PTSD. The classification accuracy is justified by a variety of different methods and metrics. **Results**: Three ANN models were established to attain the study's purpose using the susceptible regions in the right, left, and both hemispheres and the classification accuracy of ANN models achieved 79%, 93.5%, and 94.5%, respectively. The prediction accuracy even increased in the independent holdout sample using trained models. The developed models are reliable, intellectually attractive, and generalize. Additionally, the most dominant region in the PTSD individuals was the left hippocampus and the least was the right hippocampus. **Conclusion**: The present investigation achieved high classification accuracy and identified the brain regions that highly contributed to differentiating PTSD individuals from healthy controls. The results indicated that the left hippocampus is the most affected brain region in PTSD individuals. Therefore, our findings are helpful for practitioners for diagnostic, medication, and therapy of the affected brain regions by knowing the strength of infected regions.

INDEX TERMS Artificial neural network, amygdala, calibration plot, health-care, hippocampus, medial prefrontal cortex, PTSD, psychological harm, rs-fMRI, healthcare.

I. INTRODUCTION

Post-traumatic stress disorder (PTSD) is an anxiety disorder, it develops after a serious and extremely terrifying experience like domestic, school or community violence, medical trauma, disaster, war, terrorist attacks, refugee trauma, abuse, or sexual assaults [1]–[4], which may re-experience in the variety of traumatic events [5]. PTSD patients always try to avoid such circumstances and thinkings those may lead to the traumatic event, in this way they may

The associate editor coordinating the review of this manuscript and approving it for publication was Yu-Da Lin.

suffer from guilt, irritability, quarantine, dysphoria, alienation and sleep, and concentration disorder [1], [6]. In the general population, at least 7% of people fulfill the PTSD occurrence criteria at some time in their lives [7]. PTSD due to sexual assault or rape is more likely to develop than any other traumatic event [8]. Many studies also revealed the high rate of PTSD in war soldiers and war victimized [9]–[11]. At any reason for its occurrence, PTSD is a serious incapacitating health condition in itself. This disorder finally leads to disturbing the sociability, personal or family life, and become the reason for domestic violence, marital conflicts, occupational instability, and difficulties in parenting [12]. The patients with PTSD have a high association with negative thoughts that severely impair their daily lives and, intend to increase suicidal tendencies [12], [13].

PTSD prevalence is mostly observed subjectively in cross-sectional psychophysiological studies through self-reporting of symptoms, skin conductance, facial reactivity, heart rate, and such other tools [14]. Only limited studies have investigated this disorder neurologically, even the potential risk factor of PTSD development is the structural brain abnormalities [15], [16]. About the neural substrates of PTSD, many neuroimaging studies have revealed many significant findings and examined the structural changes in the brain associated with PTSD symptomatology [17]. Such vulnerable factors are supportive as accurate therapeutic and diagnosis intervention in the timely aftershock of the traumatic event to decrease the possibility of escalating chronic PTSD [18]. In recent years the imaging techniques like Positron Emission Tomography, Single Photon Emission Computed Tomography and functional Magnetic Resonance Image (fMRI) are used to examine or visualize the activation in the brain for specific regions by measuring regional Cerebral Blood Flow (rCBF), blood oxygen levels and neuroreceptor density. These activations are retrieved from the various brain regions of the PTSD patient or healthy control [19].

PTSD affects the different brain regions including the hippocampus, insula, prefrontal cortex, amygdala, medial prefrontal cortex, ventromedial prefrontal cortex, thalamus, para-hippocampus, orbitofrontal cortex, and among other brain regions [19], [20] and each region is affected at a different rate of tendency. In the pathophysiology studies of PTSD, commonly three main regions, hippocampus, medial prefrontal cortex, and amygdala are identified by substantial researches in neuroimaging. These regions involve in memory as well as in the stress response [21]. Hippocampus is presupposed in memory processes and responsible for producing context during fear conditioning [22], [23]. Hippocampus and the amygdala interact with each other during emotional memories and in the study of trauma like PTSD, the interaction between both is exceedingly relevant [24]. In the process of extinction of fear conditioning, the medial prefrontal cortex is involved and PTSD patients exhibit such fear responses in daily life [25], [26]. The third region of interest is the amygdala, which involves in the response of depression and emotional information [27], fear learning processes [28], and supportive for PTSD detection [29]. The severity of PTSD and the amygdala responses have a significant positive correlation with each other [30].

The fMRI is one of the most excellent techniques to collect brain activation data [31], even for PTSD individuals and healthy controls, it is a great source to find the activation in the regions of the brain while resting or performing a different visual, sensory and cognitive task. The resting-state fMRI (rs-fMRI) recordings are adequate to treat PTSD patients, even useful to observe the treatment response [32]. The rs-fMRI is useful for the clinical, memory, mental status investigation of the population and it provides the functional relationship between the areas of the brain [33]. Therefore, this paper only focused on the amygdala, hippocampus, and medial prefrontal cortex (brain regions) to classification of PTSD individuals from healthy control individuals using the rs-fMRI data. The present study also diagnosed the dominance level of each affected brain region in classification among the left and right regions of the hippocampus, medial prefrontal cortex and, amygdala. The classification was achieved through the Artificial Neural Network (ANN). The accurate classification between PTSD individuals and healthy controls will helpful for both neurologists and psychiatrists.

The ANN applications are enormous, ranging from voice recognition to cancer detection. Its pros outweigh the cons and make the ANN a favored modeling technique for classification, machine learning, regression, and predictions [34]. As it is flexible, reliable, fast, parametric, adaptive, multitasking, easily handle complexity in data, can handle nonlinearity of the data, can deal with a large number of inputs, no higher-level background statistics require, has the ability to decide by commenting on the similar event to learn the event, has the ability to split the problem of classification into a layered network [34]. In limited corns have been reported as time-consuming, expensive, require a lot of data for training, leads to over-fitting, hard to know how much each independent variable is influence on dependent variables [34]. However, the pros are more appealing than corns, and corns are not much serious in this advanced computing era.

ANN plays a notable role in fMRI studies for the classification and detection of the affected brain regions. Recently, Anagnostopoulou *et al.* [35] took an assessment of Autism by ANN and obtained improved results in the early diagnostic process. He *et al.* [36] used the ANN and support vector machine for the early detection of cognitive deficits in preterm infants using rs-fMRI and more robust results drawn by ANN and justified the ANN potentiality. Thomas and Chandran [37] classified the autistic and healthy control using ANN by the fMRI dataset. The classification and identification of decision-making voxels of the fMRI dataset were achieved via ANN by Ahmad, Ahmad, and Dar [38], and obtained very improved results.

Previous work on the classification of the PTSD patients and healthy controls using the rs-fMRI is limited but numerous studies worked on the same objective based on the

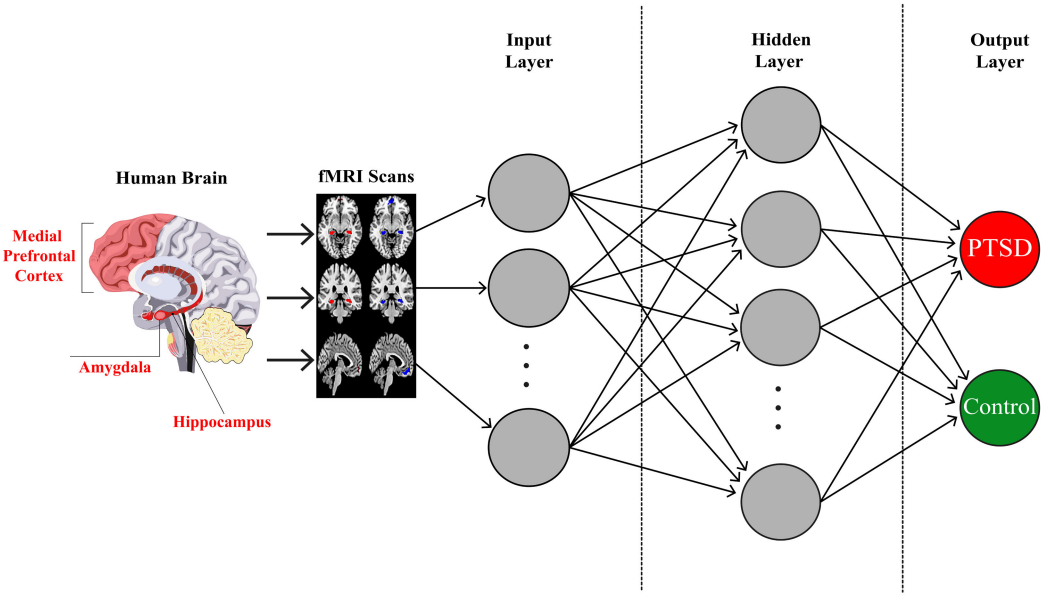

FIGURE 1. A conceptual figure to describe ANN for the present study.

survey data. In the present study, our interest is on the classification of PTSD patients and healthy controls by identifying affected brain regions using the rs-fMRI data, as neuroimaging data is more appropriate to accurate diagnoses of the brain disorder. This contribution will lead to the most relevant and efficient treatment by neurobiologists, neurologists, and psychiatrists. This was the main motivation behind considering and developing the ANN models for this study. In previous work, Christova *et al.* [39] identified the PTSD patients using neural correlation and prewhitened rs-fMRI data and found sensitivity and specificity 93.3% and 95.2%, respectively. Yuan *et al.* [40] classified the PTSD individuals with the pretreatment and posttreatment scans and obtained 72.5% accuracy by Support Vector Machine (SVM). Banerjee *et al.* [41] developed a deep belief network model and transfer learning strategy to compare with SVM, and achieved PTSD identification accuracies 61.53%, 74.99%, and 57.68%, respectively. The 42 PTSD and 39 control subjects with resting-state electroencephalogram data used in classification using linear discriminant analysis, SVM, random forest, and Fisher geodesic minimum distance to the mean approaches by Kim *et al.* [42], and 66.54%, 61.11%, 60.99%, and 75% accuracies were obtained, respectively. Similarly, Zhu *et al.* [43] investigated the multivariate pattern analysis with a relevance vector machine to classify PTSD and 89.2% accuracy was achieved to classify the PTSD. The present work expands on this previous literature, and our purposed approach will more accurately classify the PTSD subject than previous studies and additionally will reveal which region is playing the most dominant role to classify the PTSD subjects from healthy control subjects by obtaining rs-fMRI data.

The structure of this paper is as follows: Second section introduces the methodology that is used to achieve the objectives. The third section discusses the rs-fMRI data acquisition from PTSD individuals and controls in details. The fourth section presents the pre-processing of the rs-fMRI data. The data analysis and the empirical results with goodness-of-fit criteria are discussed in section fifth. The sixth section justified classification accuracy by holdout sample set, and the seventh section is for the discussion of the study. Finally, the study is concluded in the last section to make a conclusion and gives a prospect.

II. METHODOLOGY

The study aimed to develop a prediction model to classify PTSD and control individuals using rs-fMRI data. Only by observing the activation pattern in the scans of the brain visually, not leads to proper detection and classification of an individual with PTSD or a healthy control. Therefore, an advanced analysis is required to take an accurate decision, for this purpose ANN technique is considered in this study to classify the PTSD individual from the healthy control. In this way, the concerns can diagnose the disorder and treat it properly.

An artificial intelligence method that was motivated by nervous system protocol, ANN was considered and used, as sketched in Figure 1. As it is considered the best technique due to its flexibility, power, cost-effectiveness, and convenience of usage. ANNs are efficiently used in neurophysiology and robotics for solving tasks of classification [44]. The ability of ANN to model complex nonlinear relationships potentially is an attractive property for researchers. It is typically used for classification or prediction purposes in many fields, including medical and engineering as well. The formation of ANN involves one input, one or more hidden, and one output layer. The activation function and number of

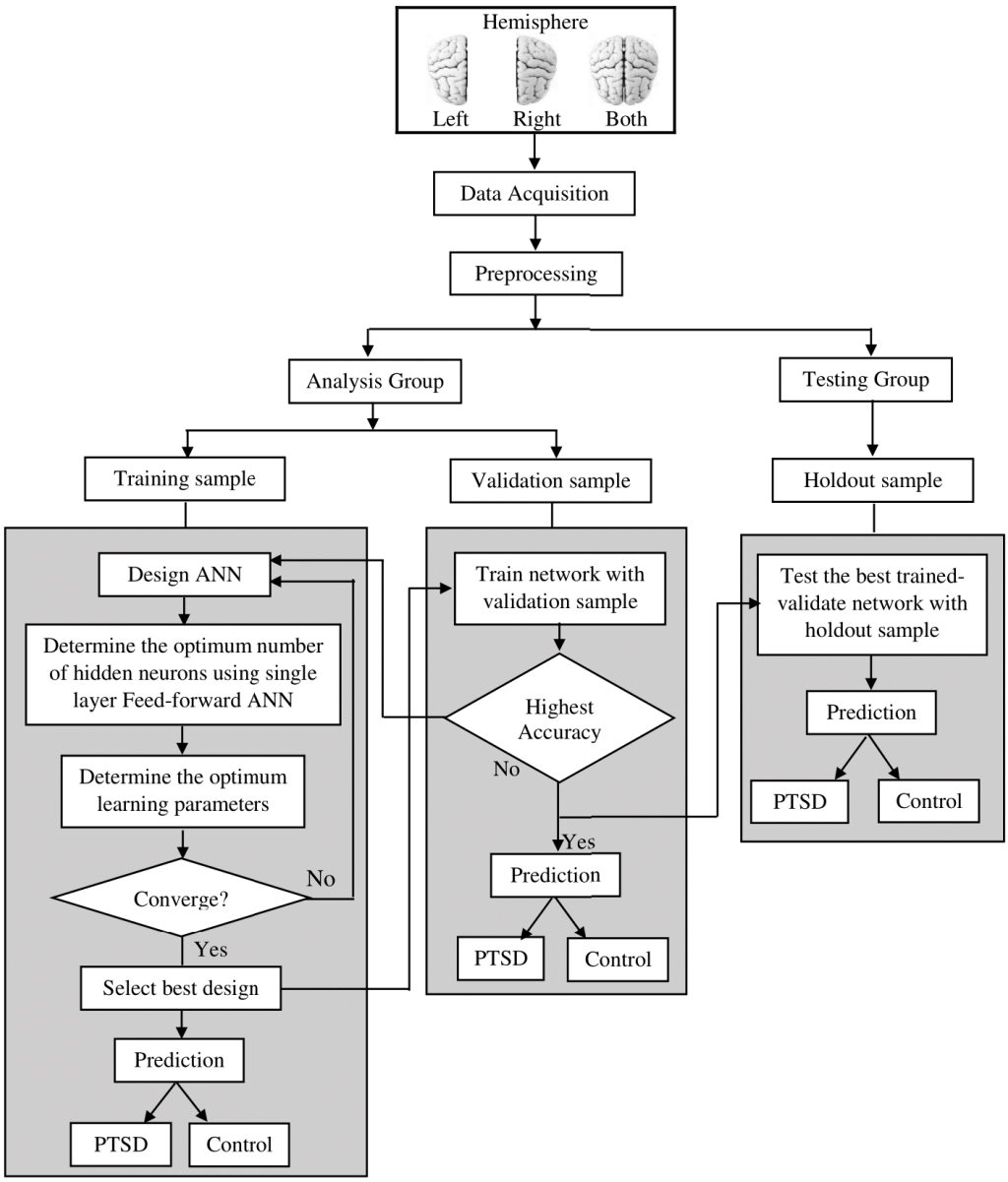

FIGURE 2. Flow-chart outline for the ANN model by considering training-validation-testing analysis approach.

units (neurons) in the hidden and output layer determines to minimize the error value using the back-propagation algorithm trial.

The training-validation-testing approach was adopted and it was implemented by splitting datasets into two groups, one group referred to the analysis group and the other as testing group. The analysis group was further divided into training and validation sample to develop the best fitted ANN models. The training sample was used to train the ANN classifier and the validation sample was used to estimate the prediction error rate of the trained ANN models. The ANN network establishes by training sample using various weights in the hidden layer and observes the output accuracy of the trained network by comparing it with the validation sample. The testing group sample, referred to as the hold-out sample that was used to test the validity of the finalized ANN models for the classification in between PTSD and healthy control, and this sample set was not involved in in-sample fitting [45]. To observe the predictive accuracy of the models, 5-fold cross-validation was employed, in order to minimize the bias associated with the random sampling of the training, validation and holdout data samples. The methodology is presented by the flowchart as in Figure 2. The sensitivity, specificity, false-positive-rate, false-negatives-rate were calculated to observe the in-depth results of the models. The receiver operating characteristic (ROC) curve was also sketched to evaluate the classification accuracy, as this curve is a plot of the sensitivity and specificity. The second goal

TABLE 1. General characteristics of patients and healthy controls.

Participants	PTSD	Control
Gender	Male	Male
Subjects	14	14
Average age	70	73.40
Participants	Veteran of the Vietnam War	Veteran of the Vietnam War
Detection	Identified by records and verified by assessment CAPS with atleast 50 score	No such record existed
rs-fMRI scans	Open eyes	Open eyes
Pre-processing scans slices	Axial (X)=64, Sagittal(Y)=64 and Coronal (Z)=48	Axial (X)=64, Sagittal (Y)=64 and Coronal (Z)=48
Post-processing scans slices	Axial (X)=75, Sagittal(Y)=95 and Coronal (Z)=79	Axial (X)=75, Sagittal(Y)=95 and Coronal (Z)=79
Inclusion Criteria	History of head trauma associated with injury, cognitive complaints, or loss of consciousness for more than 5 minutes	Comparable in age, gender, and education with PTSD groups
Exclusion Criteria	Mild cognitive dementia, history of bipolar, psychosis, stroke, hypersensitivity, alcohol, Aneurysm clips, metal implants and/or claustrophobia. Unstable major medical condition And any illness affecting brain function	

was to rank the affected brain regions associated with PTSD and contributed most to the classification; such results were obtained by the ANN model using the normalized importance graph. Finally, the activated voxels values of one PTSD and one healthy control's brain were used to evaluate the suggested model in the holdout sample as real-time analysis.

In literature, some researchers concluded that the regions in the left hemisphere affected more than the regions in the right hemisphere, due to PTSD. Therefore, this study obtained the rs-fMRI data of the hippocampus, amygdala, and medial prefrontal cortex brain regions from both left and right hemispheres to justify the most disturbing hemisphere and the brain region. Additionally, the data of both hemispheres were combined to get the data of six brain regions to observe the classification accuracy with the tendency level of each affected brain region. In this way, three datasets were in hand for the correct identification and classification of the PTSD individual and healthy control by applying three times ANN analysis. In the first ANN model, three regions-of-interest (right amygdala, right hippocampus, and right medial prefrontal cortex) of the right hemisphere were taken as input variables and named as ANN_{RH}, in the second ANN three regions (left amygdala, left hippocampus, and left medial prefrontal cortex) of the left hemisphere were taken as input variables and named as ANN_{LH} and in the third ANN, the mentioned six regions of both hemispheres were considered as independent variables and denoted by the model ANN_{BHs}. In all three models, the binary variable (PTSD individual or healthy control) is considered as a dependent variable. In this study, 14 PTSD and 14 healthy controls were selected for the analysis. A total of 28 subjects were distributed into three groups for the training, validation, and testing sample. The scans of randomly selected 9 PTSD and 9 healthy controls, 1260 (almost 64% of the total scans) used as a training sample. The activated scans of randomly selected 4 PTSD and 4 healthy controls, 560 (almost 29% of the total scans) were taken as validation sample without omitting any data unit. And remaining 2 subjects (1 PTSD and 1 healthy control) were in the testing group and their 140, 70 scans of PTSD and 70 scans of healthy (almost 8% of the total scans) holdout for the evaluation of the prediction accuracy of the models.

III. DATA ACQUISITION

A recent large study conducted by the Department of Defense and Alzheimer's Disease Neuroimaging Initiative (DoDADNI) on elder Veterans and healthy controls, those were served in Vietnam. The data was obtained from the DoDADNI [46] and the detailed description of the participants is given in Table 1. To get access to the DoDADNI datasets, we applied for that and on the acceptance of the request, the access was granted on the well-defined protocols. Then for the present study, only the PTSD individuals and healthy controls were targeted from that database. A sample of PTSD individuals and healthy controls has been sampled according to the reliability criteria. Therefore, rs-fMRI (open eyes) scans were retrieved from 14 PTSD and 14 control males with an average age of 70.00 and 73.40 years, respectively. Other characteristics of the individuals are explained in Table 1. Moreover, the PTSD brain scans had the properties like, field strength = 3.0 tesla, flip angle = 90.0 degree, manufacturer = GE medical systems, matrix X = 64.0 pixels, matrix Y = 64.0 pixels, mfg Model = discovery mr750, pixel spacing X = 3.2813mm, pixel spacing Y = 3.2813mm, pulse sequence = EP/GR, slices = 5952.0, slice thickness = 3.2999mm, TE = 30.0ms and TR = 2900.0ms. The rs-fMRI scans of controls had the same properties as mentioned above for the PTSD individuals. Each PTSD and each healthy control individual have 140 scans and every scan has 48 slices with axial view slices. The rs-fMRI data were retrieved for six regions, three from each hemisphere of the brain named the hippocampus, medial prefrontal cortex, and amygdala.

IV. DATA PRE-PROCESSING

The standard way was adopted to pre-process and analyze the rs-fMRI data by MATLAB (2018) and SPM-12 packages. In pre-processing the rs-fMRI scans were reorientation, smoothed, realigned, normalized, and slice-timing corrected, before the statistical analysis. To remove the respiratory

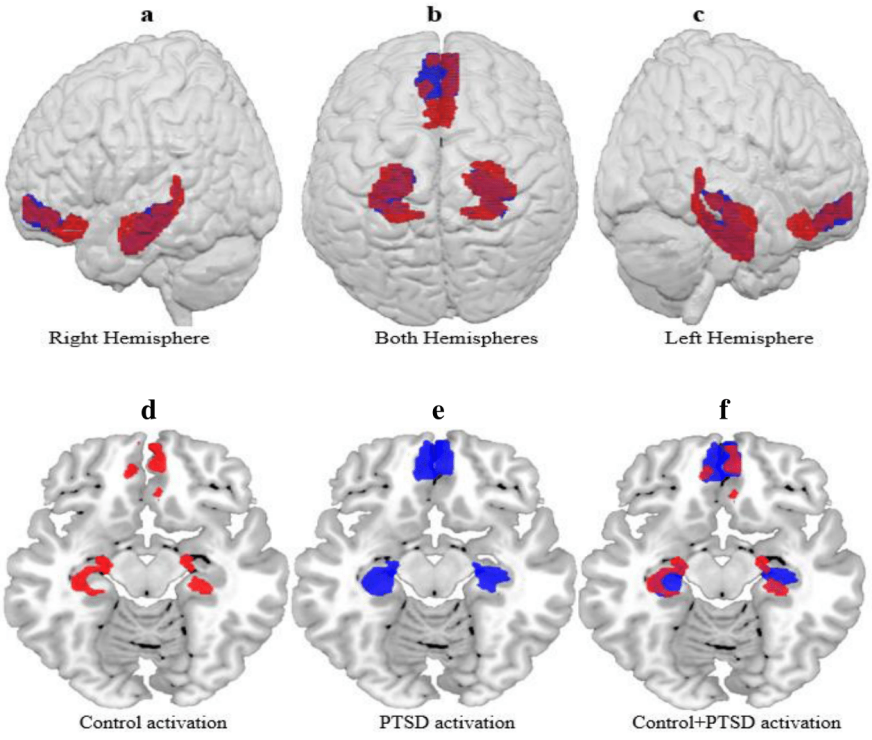

FIGURE 3. Subfigure 3a, 3b, and 3c are showing the activation in the right, both and left hemispheres, respectively. Subfigure 3d, 3e, and 3f are indicating the activation of the healthy control, PTSD individual and both, respectively, in the regions-of-interest (amygdala, hippocampus, and medial prefrontal cortex) in axial view; whereas the activation with blue color for the PTSD individuals, red color for healthy control and pink color for both individuals.

frequency noise, the 0-0.2 Hz cutoff frequency of the filter was used. The pre-processed scans were analyzed to detect the activation in the selected brain regions by taking the model specification, estimation, and results steps. The block design and all 140 scans were used in the step of the *model specification* to specify the visual conditions of PTSD individual and healthy control. Initially, the total rs-fMRI scans were $(14 + 14) \times 140 = 3920$ and after applying block design on 140 rs-fMRI scans, the activated scans $(14 + 14) \times 70 = 1960$ were obtained. The next step after the completion of the *model specification* was the *estimation*, in this step, the SPM.mat file was used to estimate the betas of every condition. In the third step *results*; contracts were used for the comparison of the beta scans with the t-test. As usual, only the contrasts with a sum to zero were considered.

Next, the activation of the voxels in the brains' regions-of-interest of the PTSD individuals and healthy controls were highlighted by specifying the threshold value as shown in Figure 3 with the different colors. Where the Sub-figure 3a presents activation in the right hemisphere, Sub-figure 3b shows activation in both hemispheres and Sub-figure 3c presents activation in the left hemisphere. In these sub-figures, the blue color indicates the activation in the brain of PTSD individuals, the red color shows activation in the brain of healthy controls and pink specifies the activation in the brain of both PTSD individuals and healthy control. Sub-figure 3d highlights the activation in the amygdala, hippocampus, and medial prefrontal cortex regions of healthy control, and similarly in Sub-figure 3e highlights the activation in brain of PTSD individuals. The activation in the brain of both PTSD and control is presented in Sub-figure 3f for comparison.

To compare the activation of the regions-of-interest (Amygdala, Hippocampus, and Medial prefrontal cortex), we made the multislice view for healthy control and PTSD individual as given in Figure 4.

V. ANALYSIS AND RESULTS

In this study, ANN with 5-fold cross-validation approach has been employed to compare the performance of the developed models using the rs-fMRI data of the selected brain regions. After the bifurcation of the data in three samples, the ANN was applied by following the steps given in Figure 2. The cross-validation classification accuracy of all the models for training and validation sample, for every fold and the average accuracy of all 5-folds are given in Table 2. Only the average results of the 5-folds cross-validation have been used for interpretation and comparison purpose in the next text. It is clear from the average results in Table 2 that the ANN_{BHs} provided the best accuracy, while ANN_{RH} gives the lowest

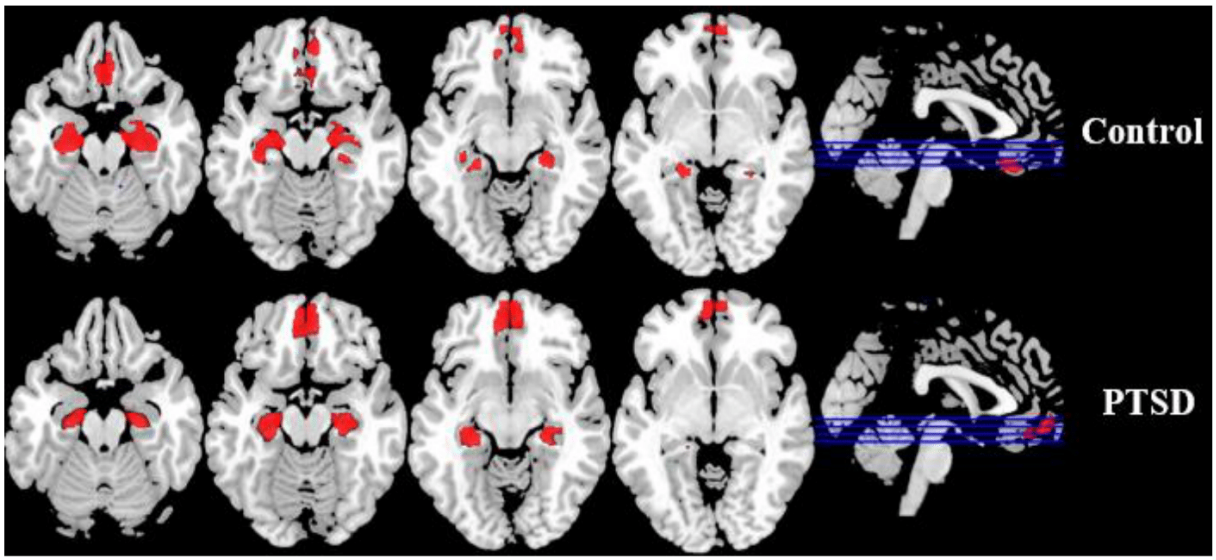

FIGURE 4. Red color shows the activation of the brain regions (amygdala, hippocampus, and medial prefrontal cortex) in a multi-slice view of PTSD individual and healthy control.

TABLE 2. The classification accuracy in percentage of 5-fold cross-validation for training and validation sample.

Model	Sample	Accuracy (%)					
		1-fold	2-fold	3-fold	4-fold	5-fold	Average
ANN_{RH}	Training	0.776	0.764	0.792	0.803	0.771	78.12
	Validation	0.75	0.714	0.786	0.788	0.964	80.04
ANN_{LH}	Training	0.941	0.965	0.954	0.912	0.935	94.14
	Validation	0.926	0.923	0.934	0.941	0.927	93.02
ANN_{BHs}	Training	0.952	0.967	0.952	0.949	0.929	94.98
	Validation	0.917	0.915	0.964	0.939	0.971	94.12

accuracy percentage, and the accuracy results of ANN_{LH} are very close to the ANN_{BHs}.

Graphically, the detailed classification results are presented in Figure 5. As the final selected ANN models efficiently classifying the PTSD individuals and healthy controls by taking rs-fMRI data of the activations in brain regions as input and produce results of the classification as output. In Figure 5, the correctly classified numbers and percentages of the scans of the region-of-interest have been appeared as the diagonal values and opposite (incorrect) classified scans are the off-diagonal values for both the training and validation samples. The overall accuracy with the regions in the right, left, and both hemispheres of the training and validation model of ANN is also shown in Figure 5. The accuracy of ANN_{RH} with the training and validation sample was 78.0% and 80%, in this way, ANN_{RH} predicted seventy-eight and eighty correct decisions out of 100, respectively. The total accuracy of ANN_{LH} with the regions in the left hemisphere by the training and validation sample was 94% and 93%, which means that our model predicted ninety-four and ninety-three correct decisions out of 100, respectively. Similarly, the correct predictions by the ANN_{BHs} with the training and validation sample were 95% and 94%, comparatively, this model provided almost the same prediction accuracy as the model with the regions in the left hemisphere and it predicted ninety-four and ninety-five correct decisions out of 100 in training and validation sample.

The training and validation loss and accuracy were measured and plotted against the first 30 epochs for ANN_{BHs}, ANN_{LH}, and ANN_{RH} model in Figure 6 with three plots, respectively. These three exemplary plots depicting the changes in training and validation loss were large initially but over the epochs, the loss decreasing gradually during the first 25 epochs and become stable after around 25 epochs for all ANN models, when the maximum 200 epochs had been executed. The ANN_{BHs} have less loss and greater accuracy as compare to the ANN_{LH} and ANN_{RH} models, similarly, ANN_{LH} have less loss and greater accuracy than ANN_{RH}. The loss for training and validation group data decayed after each epoch but ANN_{RH} has more and fluctuated loss which means that its parameters of the network did not converges to better ones model this is also reflected from the accuracy curve. The final classification accuracy on the training and validation group data were obtained as mentioned above. The best models which achieved the highest accuracy and minimum loss on the training and validation group data were reserved for testing group data.

A. HOSMER-LEMESHOW TEST

It is better to evaluate the model fitness as far as possible before relying upon it to draw a conclusion or prediction. In this regard, the popular Hosmer-Lemeshow test for binary outcomes was considered. Hosmer-Lemeshow test suggests the goodness-of-fit of the model using the observed and predicted values and it depends on the chi-square goodness-of-fit test. The insignificance of the test indicates that the model is good-fitted [47]. The results of the Hosmer-Lemeshow test in Table 3 indicate the ANN_{RH}, ANN_{LH}, and ANN_{BHs} are well-fitted models to the data as all the p-values are

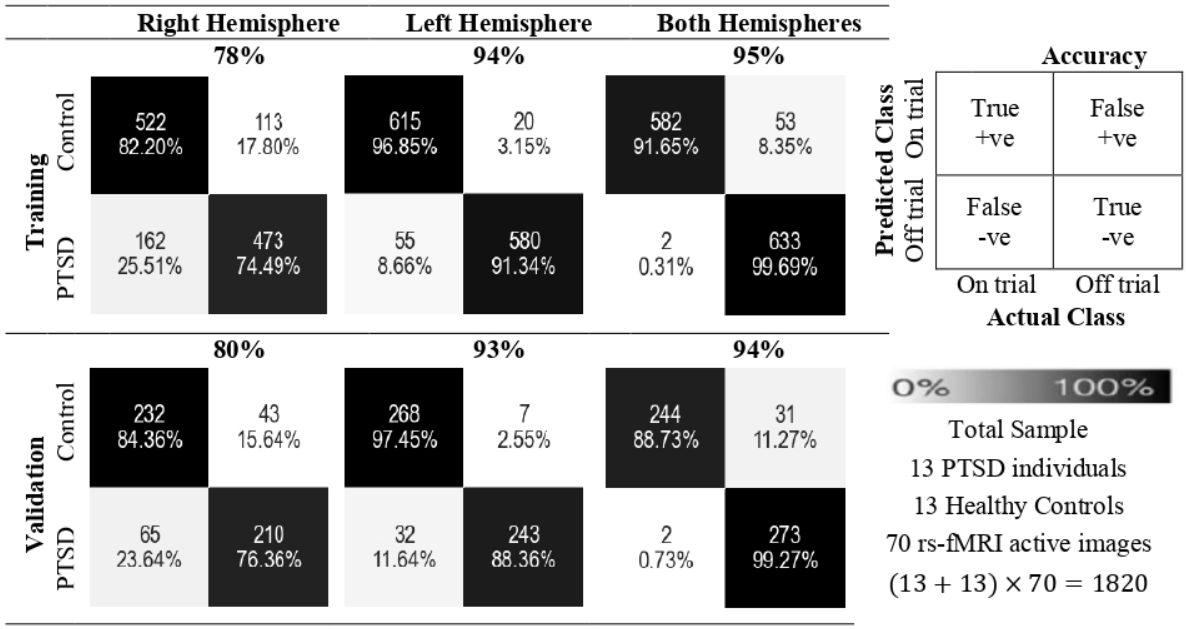

FIGURE 5. ANN classification accuracy for both training and validation sample settled during the classification of the PTSD and healthy control by the rs-fMRI scans of the brain regions in right, left, and both hemispheres. In each 2 × 2 confusion matrix, the diagonal values indicate the right decision and off-diagonal indicates wrong decisions of predictions for both the training and validation samples. The darkness of the cells of the confusion matrix increases as classification accuracy increases.

TABLE 3. Hosmer-Lemeshow test results for the three models.

Model	Chi-square	df	Sig.
ANN_{RH}	2.6538	8	0.9542
ANN_{LH}	1.2395	8	0.9962
ANN_{BHs}	0.3596	8	1.0000

very close to one. Therefore, these ANN models can predict PTSD and Control subjects accurately. Comparatively, ANN_{LH} and ANN_{BHs} are the better choices for the prediction and classification.

B. CALIBRATION PLOT

The performance of the proposed ANN model can further be quantified in terms of calibration plots. Calibration indicates the contract between observed outcomes and predicted probabilities and assess graphically how accurate the models predict [48], [49]. In the case of ideal calibration, predictions appear exactly on the diagonal line with the zero value of intercept and the value of the slope close to 1.22 along with the p-value less than 0.05 for the statistical significance. The calibration plots for the ANN_{RH}, ANN_{LH} and ANN_{BHs} models were plotted as given in Figure 7. The diagonal line refers to the perfect calibration and it is used to compare our calibrated ANN_{RH}, ANN_{LH}, and ANN_{BHs} models with dotted lines. The lines of ANN_{RH}, ANN_{LH}, and ANN_{BHs} models are close to the diagonal line. The calibration intercept for the ANN_{RH} model is 0.10 (p-value 0.012) and the calibration slope is 0.81 (p-value 0.000). The ANN_{LH} have −0.08 (p-value 0.026) value of intercept and slope is the 1.16 (p-value 0.000). The calibration intercept and slope of the ANN_{BHs} model is −0.07 (p-value 0.014) and 1.13 (p-value 0.000), respectively. The calibration curve of ANN_{RH} model deviates more from the ideal calibration line than ANN_{LH} and ANN_{BHs} models. As the calibration curve of the ANN_{LH} and ANN_{BHs} models are approximately close to the perfectly calibrated line. Therefore, the intercepts and slopes are statistically significant and very close to the benchmark values.

C. SENSITIVITY ANALYSIS

To assess more about the accuracy of the ANN models for the classification of PTSD and healthy control, we have calculated sensitivity, specificity, false-positive-rate, false-negatives-rate, and area under the ROC curve with confidence intervals. Here, sensitivity is the ability to correctly identify the PTSD individual when the individual has truly PTSD and specificity is the ability to correctly identify the healthy control individual when the individual truly healthy. The false-positive-rate is the probability that an individual is a healthy control and the model declares it PTSD individual. The false-negative-rate is the probability that an individual has PTSD and the model identifies it as healthy control. These measures are computed for training and validation sample sets separately as reported in Table 4 and overall the results are also obtained for ANN_{RH}, ANN_{LH}, and ANN_{BHs} models. Comparatively, the ability of sensitivity of ANN_{LH} model is the highest as 96.94%. It can correctly identify 96.94% of the individual who possesses PTSD. The ANN_{BHs} model has top specificity and able to correctly identify 98.42% of individual those are healthy control. The least false-positive-rate and false-negative-rate possess by the ANN_{LH}

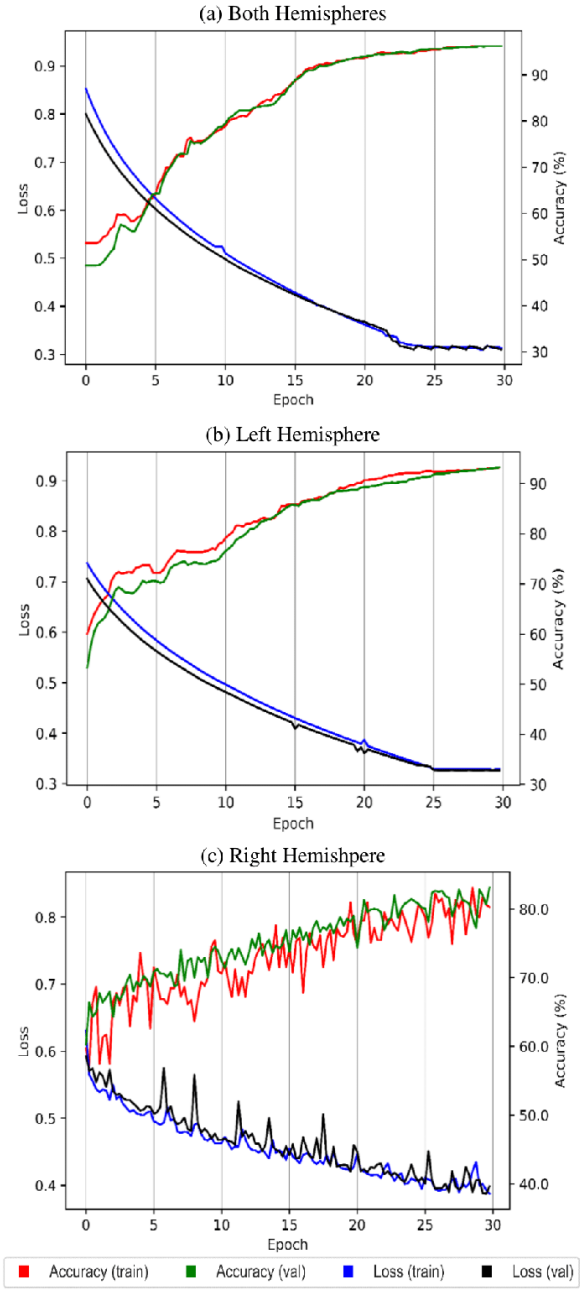

FIGURE 6. Training and validation loss and accuracy curves over epochs for ANN_{BHs}, ANN_{LH}, and ANN_{RH}.

and ANN_{BHs}, respectively, the least value of these two measures are most demanding. Since concerning the sensitivity and false-positive-rate, and whereas specificity and false-negative-rate the ANN_{LH} and ANN_{BHs} are useful and valid, respectively.

D. ROC CURVE ANALYSIS

To observe the precision of the ANN models and to display the discriminatory ability to correctly pick up PTSD and healthy controls the ROC curve analysis was performed. ROC curve is also used to provide a high degree of specificity, sensitivity, and high test-retest stability [50]. The area under

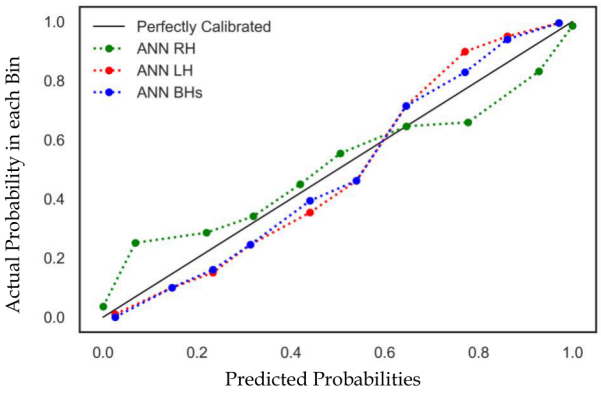

FIGURE 7. Calibration plot of the ANN models.

the ROC curve is an effective measure to diagnose the classification accuracy. According to DeSalvo *et al.* [51], ROC curve values between 0.70 and 0.80 are acceptable, ones greater than 0.80 are excellent, and ones higher than 0.90 are rarely observed. The ROC curves of the ANN models based on the regions of the right hemisphere, left hemisphere and both hemispheres are presented in Figure 8. The two lines in each the ROC curve denoted the two different classes; wherein the solid line represents the PTSD individuals and the dotted line for the healthy controls. In the training and validation sample set, the area under the ROC curves for ANN_{RH} model are obtained 0.871 and 0.883; for ANN_{LH} model 0.977 and 0.984; and for ANN_{BHs} model 0.984 and 0.984, respectively. Overall, the area under the ROC curve for the ANN_{RH}, ANN_{LH}, and ANN_{BHs} is 0.877, 0.980, and 0.984, respectively, as reported in Table 4 The comparison shows regions in the left hemisphere can clearly distinguish between PTSD individual and healthy control and even the scanning of the left hemisphere is enough to diagnose PTSD in a person. Overall, the area under the ROC (AUROC) curve of ANN_{LH} and ANN_{BHs} is very close and high.

The dominance level of each region in classification is also presented graphically in Figure 8, corresponding to the ROC curves with their respective model. In the ANN_{RH} the most important region is the right amygdala and the least important is the right hippocampus in the classification. The ANN_{LH} model that is based on the regions in the left hemisphere highlighted the left hippocampus as the most important and left amygdala as the least important. The third model ANN_{BHs} was performed with all considered six regions then the left hippocampus is the region that has the most dominant role in classification and the least is the right hippocampus. The importance of each region in classification is attained by the normalized importance graph of ANN, more the importance of a region means that the region contributes much to identify the PTSD patient.

E. COMPUTATIONAL TIME

The computational time of our developed ANN models was measured in Python language with "time" package

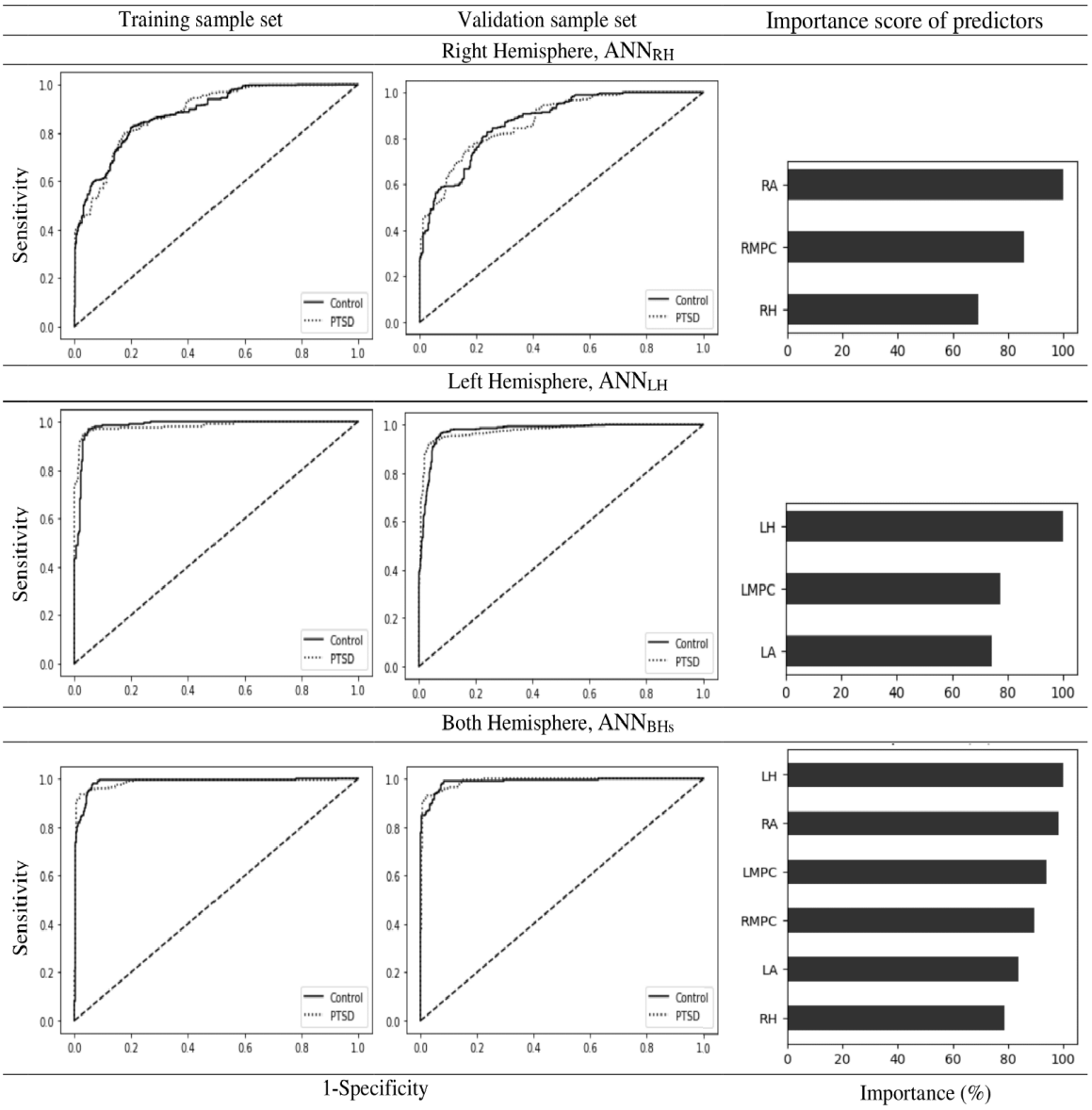

FIGURE 8. ROC curves representing sensitivity analysis of ANN models and the bar display the dominance level (in %) of affected regions in the classification of PTSD and healthy control.

TABLE 4. Sensitivity, Specificity, false-positive rate (FPR), false-negative rate (FNR) and AUROC with 95% confidence interval.

ANN Model	Sample Set	Specificity (%)	Sensitivity (%)	FPR (%)	FNR (%)	AUROC (95% CI)
ANN_{RH}	Training	79.45	77.31	20.55	22.69	0.871(0.858-0.895)
	Validation	83.00	78.11	17.00	21.89	0.883(0.878-0.903)
	Overall	81.22	77.71	18.77	22.29	0.877(0.868-0.899)
ANN_{LH}	Training	96.67	91.79	3.333	8.21	0.977(0.970-0.981)
	Validation	97.20	89.33	2.800	10.67	0.984(0.980-0.991)
	Overall	96.94	89.33	3.07	9.44	0.980(0.975-0.986)
ANN_{BHs}	Training	92.27	99.66	7.726	0.34	0.984(0.980-0.994)
	Validation	89.80	99.19	10.20	0.81	0.984(0.980-0.993)
	Overall	91.03	99.42	8.963	0.575	0.984(0.980-0.994)

using personal computer which had specifications of Intel(R) Core(TM) i5-4300M CPU @ 2.60GHz 2.60 GHz with 8 GB RAM. The computational time which was consumed in development of the ANN_{LH}, ANN_{RH} and ANN_{BHs} models with 30 epochs were 2.91, 1.88 and 2.56 seconds, respectively.

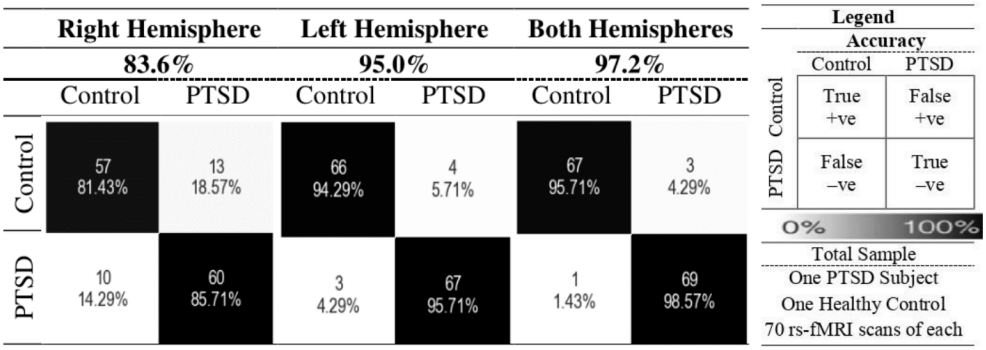

FIGURE 9. Classification matrix with accuracy in holdout sample using validated models sing affected brain regions.

VI. ANN CLASSIFICATION PERFORMANCE ON THE HOLDOUT SAMPLE

The classification performance efficiency was also tested by applying the trained and validated model on the independent holdout sample. In the holdout sample, the already recruited rs-fMRI 70 scans of a PTSD individual and 70 scans of healthy control were obtained for the experimentation to get the trust of the practitioners on the results of this study. The actual number of scans of the activated voxels of PTSD individuals in the holdout sample was 70, however, 60, 67, and 69 scans were correctly classified by ANN_{RH}, ANN_{LH}, and ANN_{BHs} model, respectively. And the actual number of scans of the activated voxels of healthy control in the holdout sample was also 70, however, 57, 66, and 67 scans were correctly classified by ANN_{RH}, ANN_{LH}, and ANN_{BHs} model, respectively. The prediction accuracy of the developed ANN_{RH}, ANN_{LH} and ANN_{BHs} model using holdout sample was achieved 83.57%, 95%, and 97.14%, respectively. The overall and individual classification accuracy of the PTSD or healthy control for all models presented in Figure 9 using the holdout sample. Comparatively, the prediction accuracy on the holdout sample increased and more accurately predicted PTSD individual and healthy control for all the models. The performance of the proposed approach validates that the rs-fMRI scans of selected brain regions have the potential to identify persons with PTSD.

VII. DISCUSSION

The practitioners required an easy and reliable method for diagnosing PTSD in an individual with full of confidence, and this study tried and achieved the desired results. As the numerous fMRI studies only studied and observed the intensity of changes in the brain of PTSD rather than focused on the classification of PTSD and healthy control. It is also observed, the neuroimaging studies investigated changing activities in only one or more than one region among left hippocampus, right hippocampus, left amygdala, right amygdala, left medial prefrontal cortex and right medial prefrontal cortex. In our study, all these six susceptible regions of the brain were considered while analyzing rs-fMRI scans to classify the PTSD individual from a healthy control. After extracting the data of the affected brain regions by SPM12 software, the ANN used for classification and prediction of the person with or without the disorder, and the identification of the regions which played the most dominant role in classifying the PTSD patient and healthy control. As the biological neural networks formation based ANN has become an efficient problem solver in medical science and extensively used for classification and prediction of medical diseases [52].

The ANN has applied separately on left, right, and both hemispheres, using the data of regions of interest as independent variables. The findings of ANN_{LH} that is based on three regions in the left hemisphere efficiently able to diagnose the PTSD patient as compared to the model ANN_{RH} with the rs-fMRI data of the three regions in the right hemisphere. As the results of the ANN_{LH} model showed more classification accuracy that the ANN_{RH}. The involvement of left hemisphere in PTSD is also justified by Baldacara *et al.* [53]. In left-hemisphere, 2.25-fold more increased abnormalities were found than right-hemisphere in PTSD by Ito *et al.* [54]. Durkee *et al.* [55] also suggesting right-hemisphere dysfunction is less than the left-hemisphere in PTSD. If only concentrate on the regions of right hemisphere, then the normalized importance graph of ANN indicated that the right amygdala is the most dominant region in classification. The most dominant region means that the region affected much due to PTSD and contributes significantly to identify the PTSD patient. It is also observed that the right medial prefrontal cortex less and the right hippocampus is the least affected region. Similarly, the normalized importance graph of ANN for left hemisphere indicated that the most prominently involved region is the left hippocampus and the least affected region is the left amygdala in the brain of PTSD patients.

The results of the third ANN model based on the six regions have the highest accuracy (94.5%) and the normalized importance graph demonstrated that the left hippocampus is the most affected region in PTSD patients. The second most affected region is the right amygdala. Respectively, the left medial prefrontal cortex, right medial prefrontal cortex, and left amygdala has decreasing effective strength. The least affected region among the affected regions is the right hippocampus. Therefore, left hippocampus is a core region that affected much in PTSD, as it is also concluded in the

case-control fMRI study of Thomaes *et al.* [56], and also justified in the meta-analysis of 37 studies by Nelson and Tumpap [57]. The right hippocampus is the least affected region in PTSD individuals, it is also discussed by Nelson and Tumpap [57].

Finally, in our approach, we have used brain regions as independent variables in ANN and the target variable was to identify the individual with or without PTSD. According to the sensitivity, specificity, false-positive-rate, false-negatives-rate, area under the ROC curves and accuracy percentages the finalized ANN models justified and achieved the objective of the study. The ANN was also used to identify of regions that played the most dominant role while classification between PTSD individual and healthy control. Additionally, this approach found out the affected regions in the brain with their strength of being infected. Ultimately, our findings are helpful for neurobiologists, neurologists, and psychiatrists for the diagnostic and treatment of PTSD individuals, even doctors can do the therapy of the affected regions by knowing the strength of infected regions.

In summary, this study is an important step toward the clinical diagnosis of PTSD with the help of ANN. However, this study does have some limitations. First, as the data of our study was related to only army personals and the general public with trauma is not the part, we urge caution when generalizing these results to other traumatic events, this study can be extended and conduct the research on the particular traumatic event fMRI data. Second, we used resting-state fMRI data to extract classification features, it may be possible to explore the results on activity-based fMRI data. Third, our study took the recommended affected brain regions in PTSD, and in the future, more regions can take which may improve the classification accuracy. Fourth, the present study is appropriate for the small and moderate sample sizes and it needs to test this methodology for a very large sample size to generalize the results for every sample size. At last, our research only compared PTSD with healthy controls, other related psychiatric disorders are not considered, and it is possible to take the data of different psychiatric disorders at once to diagnose PTSD.

VIII. CONCLUSION

In this case-control rs-fMRI study the ANN training-validation-testing approach was applied by taking six most susceptible brain regions to classify and predict the PTSD individual and to identify the dominance level of each affected brain region in the development of PTSD. As it is important to accurately diagnose PTSD individuals for the most relevant treatment in this complex stress-related psychiatric disorder. In this regard, ANN is a simple and efficient way of identification and classification. Consequently, the findings of the ANN significantly identify the affected regions and classify PTSD from healthy control with 79%, 93.5%, and 94.5%, using the regions in the right hemisphere, left hemisphere, and both hemispheres, respectively. Furthermore, the most affected region of the brain in PTSD is the left hippocampus and the least involved region is the right hippocampus, particularly, these results are consistent with many fMRI studies. The performance validation results clearly validated the appropriateness of the ANN model and selected brain regions. Our all findings will helpful for classifying the PTSD individual from healthy control with confidence and identify the affected region for most relevant intervention and treatment, such as psychotherapy or pharmacological interventions aiming to get the normal activation of the disturbed regions.

ACKNOWLEDGMENT

The authors would like to acknowledge the support of Prince Sultan University for paying the APC of this publication.

REFERENCES

[1] O. B. Yonis, Y. Khader, A. Jarboua, M. M. Al-Bsoul, N. Al-Akour, M. A. Alfaqih, M. M. Khatatbeh, and B. Amarneh, "Post-traumatic stress disorder among Syrian adolescent refugees in Jordan," *J. Public Health*, vol. 42, no. 2, pp. 319–324, May 2020.
[2] G. C. Davis and N. Breslau, "Post-traumatic stress disorder in victims of civilian trauma and criminal violence," *Psychiatric Clinics North Amer.*, vol. 17, no. 2, pp. 289–299, Jun. 1994.
[3] H. Kienzler, "Debating war-trauma and post-traumatic stress disorder (PTSD) in an interdisciplinary arena," *Social Sci. Med.*, vol. 67, no. 2, pp. 218–227, Jul. 2008.
[4] J. A. Cohen, "Practice parameter for the assessment and treatment of children and adolescents with posttraumatic stress disorder," *J. Amer. Acad. Child Adolescent Psychiatry*, vol. 49, no. 4, pp. 414–430, Apr. 2010.
[5] C. Lemogne, "Post-traumatic stress disorder and comorbid physical conditions," *J. Psychosomatic Res.*, vol. 126, Nov. 2019, Art. no. 109818.
[6] J. A. Sumner, L. D. Kubzansky, A. L. Roberts, Q. Chen, E. B. Rimm, and K. C. Koenen, "Not all posttraumatic stress disorder symptoms are equal: Fear, dysphoria, and risk of developing hypertension in trauma-exposed women," *Psychol. Med.*, vol. 50, no. 1, pp. 38–47, Jan. 2020.
[7] R. C. Kessler, P. Berglund, O. Demler, R. Jin, K. R. Merikangas, and E. E. Walters, "Lifetime prevalence and age-of-onset distributions of DSM-IV disorders in the national comorbidity survey replication," *Arch. Gen. Psychiatry*, vol. 62, no. 6, pp. 593–602, Jun. 2005.
[8] D. J. Snipes, J. M. Calton, B. A. Green, P. B. Perrin, and E. G. Benotsch, "Rape and posttraumatic stress disorder (PTSD): Examining the mediating role of explicit sex–power beliefs for men versus women," *J. Interpersonal Violence*, vol. 32, no. 16, pp. 2453–2470, Aug. 2017.
[9] A. M. Thabet, S. S. Thabet, and P. Vostanis, "The relationship between trauma due to war, post-traumatic stress disorder and fears among palestinian children," *EC Paediatrics*, vol. 7, no. 3, pp. 171–178, Mar. 2018.
[10] M. G. Pereira, J. C. Machado, M. Pereira, C. Lopes, and S. Pedras, "Quality of life in elderly portuguese war veterans with post-traumatic stress symptoms," *Patient Rel. Outcome Measures*, vol. 10, pp. 49–58, Feb. 2019.
[11] T. L. Hafemeister and N. A. Stockey, "Last stand—The criminal responsibility of war veterans returning from iraq and afghanistan with posttraumatic stress disorder," *Ind. LJ*, vol. 85, no. 1, pp. 88–141, 2010.
[12] J. Iribarren, P. Prolo, N. Neagos, and F. Chiappelli, "Post-traumatic stress disorder: Evidence-based research for the third millennium," *Evidence-Based Complementary Alternative Med.*, vol. 2, no. 4, pp. 503–512, 2005.
[13] Q. Wang, L. Ren, W. Wang, W. Xu, and Y. Wang, "The relationship between post-traumatic stress disorder and suicidal ideation among shidu parents: The role of stigma and social support," *BMC Psychiatry*, vol. 19, no. 1, pp. 1–9, Dec. 2019.
[14] R. K. Pitman, A. M. Rasmusson, K. C. Koenen, L. M. Shin, S. P. Orr, M. W. Gilbertson, M. R. Milad, and I. Liberzonh, "Biological studies of post-traumatic stress disorder," *Nat. Rev. Neurosci.*, vol. 13, no. 11, pp. 769–787, Nov. 2012.
[15] A. Shalev, I. Liberzon, and C. Marmar, "Post-traumatic stress disorder," *N. Engl. J. Med.*, vol. 376, no. 25, pp. 2459–2469, Jun. 2017.

[16] L. Helpman, M.-F. Marin, S. Papini, X. Zhu, G. M. Sullivan, F. Schneier, M. Neria, E. Shvil, M. J. M. Aragon, J. C. Markowitz, M. A. Lindquist, T. D. Wager, M. R. Milad, and Y. Neria, "Neural changes in extinction recall following prolonged exposure treatment for PTSD: A longitudinal fMRI study," *NeuroImage, Clin.*, vol. 12, pp. 715–723, Feb. 2016.

[17] M. Boccia, S. D'Amico, F. Bianchini, A. Marano, A. M. Giannini, and L. Piccardi, "Different neural modifications underpin PTSD after different traumatic events: An fMRI meta-analytic study," *Brain Imag. Behav.*, vol. 10, no. 1, pp. 226–237, Mar. 2016.

[18] A. Y. Shalev, Y. Ankri, Y. Israeli-Shalev, T. Peleg, R. Adessky, and S. Freedman, "Prevention of posttraumatic stress disorder by early treatment: Results from the jerusalem trauma outreach and prevention study," *Arch. Gen. Psychiatry*, vol. 69, no. 2, pp. 166–176, Feb. 2012.

[19] A. Prasad, A. Chaichi, D. P. Kelley, J. Francis, and M. R. Gartia, "Current and future functional imaging techniques for post-traumatic stress disorder," *RSC Adv.*, vol. 9, no. 42, pp. 24568–24594, 2019.

[20] L. D. Selemon, K. A. Young, D. A. Cruz, and D. E. Williamson, "Frontal lobe circuitry in posttraumatic stress disorder," *Chronic Stress*, vol. 3, pp. 1–17, May 2019.

[21] J. D. Bremner, "Imaging in CNS disease states: PTSD," in *Imaging in CNS Drug Discovery and Development: Implications for Disease and Therapy*. New York, NY, USA: Springer, 2010, pp. 339–360.

[22] D. T. Acheson, J. E. Gresack, and V. B. Risbrough, "Hippocampal dysfunction effects on context memory: Possible etiology for posttraumatic stress disorder," *Neuropharmacology*, vol. 62, no. 2, pp. 674–685, Feb. 2012.

[23] R. Admon, D. Leykin, G. Lubin, V. Engert, J. Andrews, J. Pruessner, and T. Hendler, "Stress-induced reduction in hippocampal volume and connectivity with the ventromedial prefrontal cortex are related to maladaptive responses to stressful military service," *Hum. Brain Mapping*, vol. 34, no. 11, pp. 2808–2816, Nov. 2013.

[24] E. Levy-Gigiab, C. Szabó, O. Kelemen, and S. Kéri, "Association among clinical response, hippocampal volume, and FKBP5 gene expression in individuals with posttraumatic stress disorder receiving cognitive behavioral therapy," *Biol. Psychiatry*, vol. 74, no. 11, pp. 793–800, Dec. 2013.

[25] A. Karl, M. Schaefer, L. Malta, D. Dörfel, N. Rohleder, and A. Werner, "A meta-analysis of structural brain abnormalities in PTSD," *Neurosci. Biobehavioral Rev.*, vol. 30, no. 7, pp. 1004–1031, Jan. 2006.

[26] T. Kataoka, M. Fuchikami, S. Nojima, N. Nagashima, M. Araki, J. Omura, T. Miyagi, Y. Okamoto, and S. Morinobu, "Combined brain-derived neurotrophic factor with extinction training alleviate impaired fear extinction in an animal model of post-traumatic stress disorder," *Genes, Brain Behav.*, vol. 18, no. 7, Sep. 2019, Art. no. e12520.

[27] K. D. Young, V. Zotev, R. Phillips, M. Misaki, W. C. Drevets, and J. Bodurka, "Amygdala real-time functional magnetic resonance imaging neurofeedback for major depressive disorder: A review," *Psychiatry Clin. Neurosci.*, vol. 72, no. 7, pp. 466–481, Jul. 2018.

[28] R. A. Morey, E. K. Clarke, C. C. Haswell, R. D. Phillips, A. N. Clausen, M. S. Mufford, Z. Saygin, M. Brancu, J. C. Beckham, P. S. Calhoun, and E. Dedert, "Amygdala nuclei volume and shape in military veterans with posttraumatic stress disorder," *Biol. Psychiatry Cogn. Neurosci. Neuroimaging*., vol. 5, no. 3, pp. 281–290, Mar. 2020.

[29] A. A. Nicholson, D. Rabellino, M. Densmore, P. A. Frewen, C. Paret, R. Kluetsch, C. Schmahl, J. Théberge, R. W. J. Neufeld, M. C. McKinnon, J. P. Reiss, R. Jetly, and R. A. Lanius, "The neurobiology of emotion regulation in posttraumatic stress disorder: Amygdala downregulation via real-time fMRI neurofeedback," *Hum. Brain Mapping*, vol. 38, no. 1, pp. 541–560, Jan. 2017.

[30] Y. J. Kim, S. J. H. Rooij, T. D. Ely, N. Fani, K. J. Ressler, T. Jovanovic, and J. S. Stevens, "Association between posttraumatic stress disorder severity and amygdala habituation to fearful stimuli," *Depression Anxiety*, vol. 36, no. 7, pp. 647–658, Jul. 2019.

[31] K. A. Norman, S. M. Polyn, G. J. Detre, and J. V. Haxby, "Beyond mind-reading: Multi-voxel pattern analysis of fMRI data," *Trends Cognit. Sci.*, vol. 10, no. 9, pp. 424–430, Sep. 2006.

[32] P. Zhutovsky, R. Thomas, T. Varkevisser, M. Olff, S. J. H. van Rooij, M. Kennis, G. van Wingen, and E. Geuze, "Predicting trauma-focused therapy outcome from resting-state functional magnetic resonance imaging in veterans with posttraumatic stress disorder," *Biol. Psychiatry*, vol. 83, no. 9, pp. S357, May 2018.

[33] A. S. Heinsfeld, A. R. Franco, R. C. Craddock, A. Buchweitz, and F. Meneguzzi, "Identification of autism spectrum disorder using deep learning and the ABIDE dataset," *NeuroImage, Clin.*, vol. 17, pp. 16–23, Jan. 2018.

[34] G. Ciaburro and B. Venkateswaran, *Neural Networks With R: Smart Models Using CNN, RNN, Deep Learning, and Artificial Intelligence Principles*. Birmingham, U.K.: Packt, Sep. 2017.

[35] P. Anagnostopoulou, V. Alexandropoulou, G. Lorentzou, A. Lykothanasi, P. Ntaountaki, and A. Drigas, "Artificial intelligence in autism assessment," *Int. J. Emerg. Technol. Learn.*, vol. 15, no. 6, pp. 95–107, Mar. 2020.

[36] L. He, H. Li, S. K. Holland, W. Yuan, M. Altaye, and N. A. Parikh, "Early prediction of cognitive deficits in very preterm infants using functional connectome data in an artificial neural network framework," *NeuroImage, Clin.*, vol. 18, pp. 290–297, Jan. 2018.

[37] M. Thomas and A. Chandran, "Artificial neural network for diagnosing autism spectrum disorder," in *Proc. 2nd Int. Conf. Trends Electron. Informat. (ICOEI)*, May 2018, pp. 930–933.

[38] F. Ahmad, I. Ahmad, and W. M. Dar, "Identification and classification of voxels of human brain for rewardless-related decision making using ANN technique," *Neural Comput. Appl.*, vol. 28, no. S1, pp. 1035–1041, Dec. 2017.

[39] P. Christova, L. M. James, B. E. Engdahl, S. M. Lewis, and A. P. Georgopoulos, "Diagnosis of posttraumatic stress disorder (PTSD) based on correlations of prewhitened fMRI data: Outcomes and areas involved," *Exp. Brain Res.*, vol. 233, no. 9, pp. 2695–2705, Sep. 2015.

[40] M. Yuan, C. Qiu, Y. Meng, Z. Ren, C. Yuan, Y. Li, M. Gao, S. Lui, H. Zhu, Q. Gong, and W. Zhang, "Pre-treatment resting-state functional MR imaging predicts the long-term clinical outcome after short-term paroxtine treatment in post-traumatic stress disorder," *Frontiers Psychiatry*, vol. 9, p. 532, Oct. 2018.

[41] D. Banerjee, K. Islam, K. Xue, G. Mei, L. Xiao, G. Zhang, R. Xu, C. Lei, S. Ji, and J. Li, "A deep transfer learning approach for improved post-traumatic stress disorder diagnosis," *Knowl. Inf. Syst.*, vol. 60, no. 3, pp. 1693–1724, Sep. 2019.

[42] Y.-W. Kim, S. Kim, M. Shim, M. J. Jin, H. Jeon, S.-H. Lee, and C.-H. Im, "Riemannian classifier enhances the accuracy of machine-learning-based diagnosis of PTSD using resting EEG," *Prog. Neuro-Psychopharmacol. Biol. Psychiatry*, vol. 102, Aug. 2020, Art. no. 109960.

[43] H. Zhu, M. Yuan, C. Qiu, Z. Ren, Y. Li, J. Wang, X. Huang, S. Lui, Q. Gong, W. Zhang, and Y. Zhang, "Multivariate classification of earthquake survivors with post-traumatic stress disorder based on large-scale brain networks," *Acta Psychiatrica Scandinavica*, vol. 141, no. 3, pp. 285–298, Mar. 2020.

[44] A. E. Hramov, N. S. Frolov, V. A. Maksimenko, V. V. Makarov, A. A. Koronovskii, J. Garcia-Prieto, L. F. Antón-Toro, F. Maestú, and A. N. Pisarchik, "Artificial neural network detects human uncertainty," *Chaos, Interdiscipl. J. Nonlinear Sci.*, vol. 28, no. 3, Mar. 2018, Art. no. 033607.

[45] D. M. Hawkins, "The problem of overfitting," *J. Chem. Inf. Comput. Sci.*, vol. 44, no. 1, pp. 1–12, Jan. 2004.

[46] *Department of Defense (DOD) ADNI*. Accessed: Feb. 19, 2021. [Online]. Available: https://ida.loni.usc.edu/pages/access/search.jsp

[47] T. Ayer, O. Alagoz, J. Chhatwal, J. W. Shavlik, C. E. Kahn, and E. S. Burnside, "Breast cancer risk estimation with artificial neural networks revisited: Discrimination and calibration," *Cancer*, vol. 116, no. 14, pp. 3310–3321, Apr. 2010.

[48] E. W. Steyerberg, A. J. Vickers, N. R. Cook, T. Gerds, M. Gonen, N. Obuchowski, M. J. Pencina, and M. W. Kattan, "Assessing the performance of prediction models: A framework for traditional and novel measures," *Epidemiology*, vol. 21, no. 1, pp. 128–138, Jan. 2010.

[49] Z.-H. Tang, J. Liu, F. Zeng, Z. Li, X. Yu, and L. Zhou, "Comparison of prediction model for cardiovascular autonomic dysfunction using artificial neural network and logistic regression analysis," *PLoS ONE*, vol. 8, no. 8, Aug. 2013, Art. no. e70571.

[50] M.-W. Xu, H.-M. Liu, G. Tan, T. Su, C.-Q. Xiang, W. Wu, B. Li, Q. Lin, X.-W. Xu, Y.-L. Min, W.-F. Liu, G.-P. Gao, and Y. Shao, "Altered regional homogeneity in patients with corneal ulcer: A resting-state functional MRI study," *Frontiers Neurosci.*, vol. 13, pp. 1–8, Jul. 2019.

[51] K. B. DeSalvo, V. S. Fan, M. B. McDonell, and S. D. Fihn, "Predicting mortality and healthcare utilization with a single question," *Health Services Res.*, vol. 40, no. 4, pp. 1234–1246, Apr. 2005.

[52] R. Parveen, M. Nabi, F. A. Memon, S. Zaman, and M. Ali, "A review and survey of artificial neural network in medical science," *J. Adv. Res. Comput. Appl.*, vol. 3, no. 1, pp. 7–16, 2016.

[53] L. Baldaçara, A. P. Jackowski, A. Schoedl, M. Pupo, S. B. Andreoli, M. F. Mello, A. L. T. Lacerda, J. J. Mari, and R. A. Bressan, "Reduced cerebellar left hemisphere and vermal volume in adults with PTSD from a community sample," *J. Psychiatric Res.*, vol. 45, no. 12, pp. 1627–1633, Dec. 2011.

[54] Y. Ito, M. H. Teicher, C. A. Glod, D. Harper, E. Magnus, and H. A. Gelbard, "Increased prevalence of electrophysiological abnormalities in children with psychological, physical, and sexual abuse," *J. Neuropsychiatry Clin. Neurosci.*, vol. 5, no. 4, pp. 401–408, 1993.

[55] C. A. Durkee, J. E. Sarlls, D. W. Hommer, and R. Momenan, "White matter microstructure alterations: A study of alcoholics with and without post-traumatic stress disorder," *PLoS ONE*, vol. 8, no. 11, Nov. 2013, Art. no. e80952.

[56] K. Thomaes, E. Dorrepaal, N. P. J. Draijer, M. B. de Ruiter, B. M. Elzinga, A. J. van Balkom, P. L. M. Smoor, J. Smit, and D. J. Veltman, "Increased activation of the left hippocampus region in complex PTSD during encoding and recognition of emotional words: A pilot study," *Psychiatry Res., Neuroimaging*, vol. 171, no. 1, pp. 44–53, Jan. 2009.

[57] M. D. Nelson and A. M. Tumpap, "Posttraumatic stress disorder symptom severity is associated with left hippocampal volume reduction: A meta-analytic study," *CNS Spectrums*, vol. 22, no. 4, pp. 363–372, Aug. 2017.

MIRZA NAVEED SHAHZAD received the M.Sc. degree in statistics from the University of the Punjab, Lahore, Pakistan, the M.Phil./M.S. and Ph.D. degrees in statistics from Quaid-i-Azam University, Islamabad, Pakistan, in 2008 and 2016, respectively. During his Ph.D., he won the fellowship for six months and conducted research work with the Department of Mathematics and Statistics, McMaster University, Canada, and established new methods in probability. He is currently an Assistant Professor with the Department of Statistics, University of Gujrat, Pakistan. Previously, he worked as a Lecturer with UOG and GCUF, and as an Assistant Director with HEC. He has over 30 scholarly contributions in journals and conferences. His research interests include probabilistic theory, applied statistics, Bayesian statistics, time-series analysis, hybrid models, and biostatistics. He is an active reviewer of many manuscripts related to his area of interest for several international journals. He has command of a variety of subjects and taught several courses at the graduate and postgraduate levels.

HAIDER ALI received the B.S (Hons) degree from the University of Gujrat, Gujrat, Pakistan, in 2018. Now, he is a M.Phil scholar in the University of Gujrat, Gujrat, Pakistan. He has worked on two international projects as a junior data analyst. He is a well-known data analyst in his community and analyzed various types of datasets. His main research interests include neuro-statistics to analyze fMRI and MRI data through machine learning, and deep learning techniques.

TANZILA SABA (Senior Member, IEEE) received the Ph.D. degree in document information security and management from the Faculty of Computing, Universiti Teknologi Malaysia (UTM), Malaysia, in 2012. She has been nominated as a Research Professor with Prince Sultan University, Riyadh, Saudi Arabia, since September 2019. She is currently working as an Associate Chair with the Information Systems Department, College of Computer and Information Sciences, Prince Sultan University. She has above 100 publications that have around 4370 citations with H-index 42. Her mostly publications are in biomedical research published in ISI indexed. Due to her excellent research achievement, she is included in Marquis Who's Who 2012. She is an editor and a reviewer of reputed journals and on the panel of TPC of international conferences. She has full command of a variety of subjects and taught several courses at the graduate and postgraduate levels. On the accreditation side, she is a skilled lady with ABET and NCAAA quality assurance. She is the Leader of the Artificial Intelligence & Data Analytics Research Lab, PSU. Her research interests include medical imaging, pattern recognition, data mining, MRI analysis, and soft-computing. She is an Active Professional Member of ACM, AIS, and IAENG organizations. She is the PSU Women in Data Science (WiDS) Ambassador at Stanford University and Global WomenTech Conference. She received the Best Researcher Award at PSU for consecutive four years. She received the Best Student Award from the Faculty of Computing, UTM, in 2012.

AMJAD REHMAN (Senior Member, IEEE) received the Ph.D. degree (Hons.) with a specialization in forensic documents analysis and security from the Faculty of Computing, Universiti Teknologi Malaysia, in 2010. He held a postdoctoral position with the Faculty of Computing, Universiti Teknologi Malaysia, with a specialization in forensic documents analysis and security, in 2011. He is currently a Senior Researcher with the Artificial Intelligence & Data Analytics Lab, Prince Sultan University, Riyadh, Saudi Arabia. He is a PI in several funded projects and also completed projects funded from MOHE Malaysia, Saudi Arabia. He is the author of more than 200 ISI journal articles and conference papers. His research interests include data mining, health informatics, and pattern recognition. His H-index is 40 with 4000 citations. He received the Rector Award for the 2010 Best Student in the university.

HOSHANG KOLIVAND received the M.S. degree in applied mathematics and computer from Amirkabir University, Iran, in 1999, and the Ph.D. degree from the Media and Games Innovation Centre of Excellence (MaGIC-X), Universiti Teknologi Malaysia (UTM), in 2013. He held a postdoctoral position in augmented reality with UTM. Previously, he worked as a Lecturer with Shahid Beheshti University, Iran, and then as a Senior Lecturer with UTM. He is currently a Senior Lecturer with Liverpool John Moores University. He has published numerous articles in international journals, conference proceedings, and technical articles, including chapters in books. He has also published many books in object-oriented programming and mathematics. His research interests include computer graphics, virtual reality, and augmented reality. He is an active reviewer of many conference and international journals.

SAEED ALI BAHAJ received the Ph.D. degree from Pune University, India, in 2006. He is currently an Associate Professor with the Department of Computer Engineering, Hadramout University, and also an Assistant Professor with Prince Sattam Bin Abdul-Aziz University. His main research interests include artificial intelligence, information management, forecasting, information engineering, big data, and information security.